

Sintering and properties of $\text{SrBi}_2(\text{Ta}_{1-x}\text{V}_x)_2\text{O}_9$ ceramics

JIAN-JYH SHYU*, CHIH-CHUNG LEE

Department of Materials Engineering, Tatung University, Taipei 104, Taiwan, ROC

E-mail: jjshyu@ttu.edu.tw

The effects of vanadium doping on the sintering, microstructure, dielectric properties, and ferroelectric properties of $\text{SrBi}_2(\text{Ta}_{1-x}\text{V}_x)_2\text{O}_9$ ceramics were investigated. The densification and grain-growth processes of the vanadium doped ceramics were shifted to a lower temperature range. For the ceramics with relative density $\geq 90\%$, the dielectric constant is 120–125 and 100–130 for the undoped and doped ceramics, respectively, and the dielectric loss tangent is below 1%. As compared with the undoped ceramics, the ferroelectric properties can be significantly improved by doping with an appropriate amount of vanadium and sintering at 1000°C . The variations of dielectric and ferroelectric properties are influenced by the incorporation of vanadium into crystal lattice and several microstructural factors. © 2003 Kluwer Academic Publishers

1. Introduction

$\text{SrBi}_2\text{Ta}_2\text{O}_9$ (SBT) thin films have been extensively investigated as promising candidates for nonvolatile ferroelectric random access memories, because of high fatigue endurance (up to 10^{11} to 10^{12} switching cycles) and low leakage current with Pt electrodes [1–3]. However, the major disadvantages of SBT are the low remanent polarization and the high processing temperature [4, 5]. It has been reported that the properties of layered perovskite SBT ferroelectrics (thin films or ceramics) can be influenced by composition modification. According to Bhattacharyya *et al.* [6], the Bi content remarkably affects the ferroelectric properties of SBT thin films. Effects of Sr/Bi ratio on the phase formation, ferroelectric phase transition, dielectric properties, and ferroelectric properties have been investigated [7–12]. It has also been reported that the remanent polarization of SBT thin films can be improved by partial substitution of Sr^{2+} by Ba^{2+} [13].

$\text{SrBi}_2\text{Ta}_2\text{O}_9$ belongs to the Aurivillius family of bismuth layered perovskites of the general formula $(\text{Bi}_2\text{O}_2)^{2+}(\text{A}_{m-1}\text{B}_m\text{O}_{3m+1})^{2-}$, where $A = \text{Na, K, Ca, Sr, Ba, Pb, Bi, etc.}$, $B = \text{Ti}^{4+}, \text{Nb}^{5+}, \text{Ta}^{5+}, \text{Mo}^{6+}, \text{W}^{6+}, \text{Fe}^{3+}, \text{etc.}$ and $m = 1-5$ [14]. In this paper, we report on the effects of vanadium doping on the sintering, microstructure, dielectric properties, and ferroelectric properties of $\text{SrBi}_2\text{Ta}_2\text{O}_9$ in ceramic form. This study may result in materials with enhanced ferroelectric properties that are useful in applications.

2. Experimental procedures

2.1. Sample preparation

The ceramic compositions studied are $\text{SrBi}_2(\text{Ta}_{1-x}\text{V}_x)_2\text{O}_9$, where $x = 0, 0.025, 0.05, 0.075,$

0.1, and 0.2. The ceramics were prepared by standard ceramic procedure. Reagent-grade SrCO_3 , Bi_2O_3 , Ta_2O_5 , and V_2O_5 powders were mixed for 6 h in PE bottles containing yttria-stabilized zirconia balls and alcohol. After being dried, the powders were calcined at 900°C for 3 h. According to the XRD analysis, the as-calcined powders revealed a single layered perovskite phase. The powders were milled for 48 h with 5.5 wt% of polyvinyl alcohol as binder in PE bottles containing yttria-stabilized zirconia balls and alcohol. The slurries were then dried and screened (<100 mesh). The powders of 1.0 g were uniaxially pressed into disc compacts in a 10 mm diameter steel die lubricated with a thin layer of stearic acid. The powder compacts, which were embedded in the powder with the same composition in an alumina crucible with an alumina lid, were pre-fired at 550°C for 2 h, followed by sintering at $1000^\circ-1300^\circ\text{C}$ for 3 h, and then furnace cooled.

2.2. Characterization

Phase identification was conducted by X-ray diffraction (XRD) analysis on the as-sintered surface. Measurements were performed on a diffractometer (Model D5000, Siemens, Germany) with $\text{Cu } K_\alpha$ radiation. The operating power was 40 kV and 20 mA. Continuous scanning was used with a sampling interval of 0.02° (2θ). Bulk density (ρ_b) and open porosity for the sintered bodies were measured by the Archimedes method. The theoretical density (ρ_{th}) of $\text{SrBi}_2(\text{Ta}_{1-x}\text{V}_x)_2\text{O}_9$ was calculated by dividing the cell weight by the cell volume, which was estimated from lattice constants measured by XRD. Then, the relative density (ρ_r) of the sintered bodies was calculated by ρ_b/ρ_{th} . The

* Author to whom all correspondence should be addressed.

as-sintered surface of the sintered bodies, coated with a thin film of gold, was examined by scanning electron microscopy (SEM).

The dielectric constant and loss tangent of the sintered bodies were measured at the room temperature by an LCR meter (Model HP4284A, Hewlett-Packard, Tokyo, Japan) with an oscillating voltage of 1 V and a frequency of 1 kHz. The sintered samples were polished to remove a thickness of about 100 μm , then were electroded by firing a 70Ag/30Pd paint at 850°C for 30 min. For the ferroelectric loop measurement, samples were ground and polished to a thickness of >0.1 to 0.2 mm, then were gold electroded by sputtering with masked edges. The *P-E* hysteresis loops were observed at room temperature using a modified Sawyer-Tower circuit with 60 Hz sinusoidal field. The samples were dipped in silicone oil during measurement.

3. Results and discussion

3.1. Densification, X-ray analysis, and microstructure

For the ceramics doped with a lower amount of vanadium ($x = 0-0.05$), a single layered perovskite can be formed (e.g., Fig. 1a and b for $x = 0$). For the ceramics with $x = 0.075-0.2$, single layered perovskite was formed at 900°–1100°C, while a trace amount of an unknown phase also formed at 1200°–1300°C (e.g., Fig. 1c for $x = 0.2$). It was found that the lattice constants of the layered perovskite (not shown) decreased with the increase in vanadium content, indicating that vanadium has been incorporated into the lattice, although a trace amount of second phase is formed. The decrease in cell volume can be explained by the smaller ion sizes of V^{5+} than Ta^{5+} ($r_{\text{V}^{5+}} = 0.54 \text{ \AA}$ and $r_{\text{Ta}^{5+}} = 0.64 \text{ \AA}$, CN = 6 [15]). Moreover, the undoped ceramics showed a slightly increased (00 ℓ) preferred orientation of the layered perovskite at 1300°C (compare Fig. 1a with b). However, the preferred orientation became remarkable for the doped ceramics sintered at 1100°–1300°C (e.g., Fig. 1c). It was found that when the samples were polished to remove a

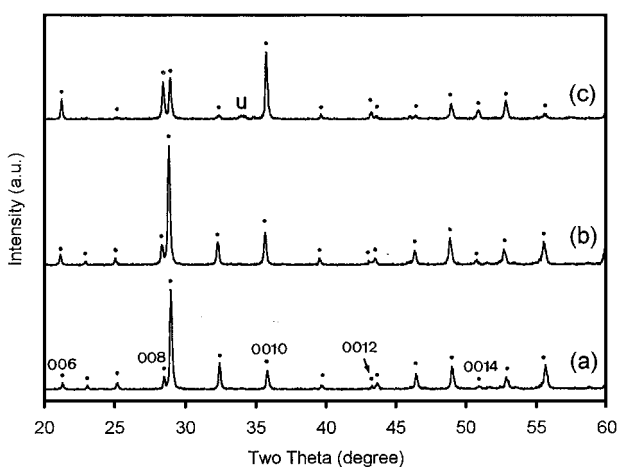


Figure 1 Typical XRD patterns of the sintered ceramics (●: layered perovskite, u: unknown). (a) $x = 0$, sintered at 1200°C, (b) $x = 0$, sintered at 1300°C, (c) $x = 0.2$, sintered at 1300°C.

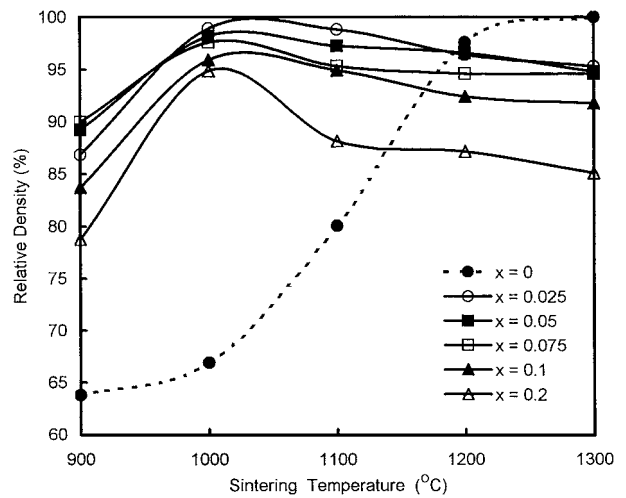


Figure 2 Relative density of the ceramics as a function of sintering temperature.

thickness of about 0.4 mm, the preferred orientation vanished.

Fig. 2 shows the degree of densification (represented by relative density) of the sintered samples. The relative density of the undoped composition increased in the temperature range 900°–1200°C, then approached about 97–99.9% at 1200°–1300°C. For the doped compositions, the densification curve was remarkably shifted to a lower temperature range, possibly due to liquid-phase sintering because of the low-temperature eutectic in the SrO-V₂O₅ system [16]. Moreover, all the doped compositions showed a maximum densification at 1000°C, followed by a density reduction. As a result, as compared with the undoped composition, the densification was improved when the sintering temperature was $\leq 1100^\circ\text{C}$, while the densification was reduced when the sintering temperature was $\geq 1200^\circ\text{C}$. It can also be seen that the densification for the doped compositions decreased with the increase in the vanadium content. A relative density of $\geq 90\%$ can be obtained for the ceramics with $x = 0$ sintered at $\geq 1200^\circ\text{C}$, $x = 0.025-0.05$ sintered at $\geq 900^\circ\text{C}$, $x = 0.075-0.1$ sintered at $\geq 1000^\circ\text{C}$, or $x = 0.2$ sintered at 1000°C.

The average grain size of the undoped ceramics increased smoothly when the sintering temperature was increased from 900°C to 1300°C (Fig. 3a–d). The microstructure consists of nearly equiaxed grains at temperatures $\leq 1100^\circ\text{C}$. The grain size is about 0.5–1 μm at 1100°C. When the sintering temperature was increased to 1200°–1300°C, several plate-like grains developed. The aspect ratio of the plate-like grains is about 2.5–4 at 1300°C. For all the doped ceramics, the temperature at which the plate-like grains developed reduced to 1000°C (see Fig. 4a for $x = 0.05$). When the sintering temperature is increased to 1100°C, almost all the grains are plate-like (see Fig. 4b for $x = 0.05$). Moreover, the average grain-size and the aspect ratio of the plate-like grains increased abruptly. The microstructure became more coarse when the sintering temperature was further increased, as seen in Fig. 4c and d. With the increase in the vanadium content, the average grain-size is nearly constant when the sintering temperature is

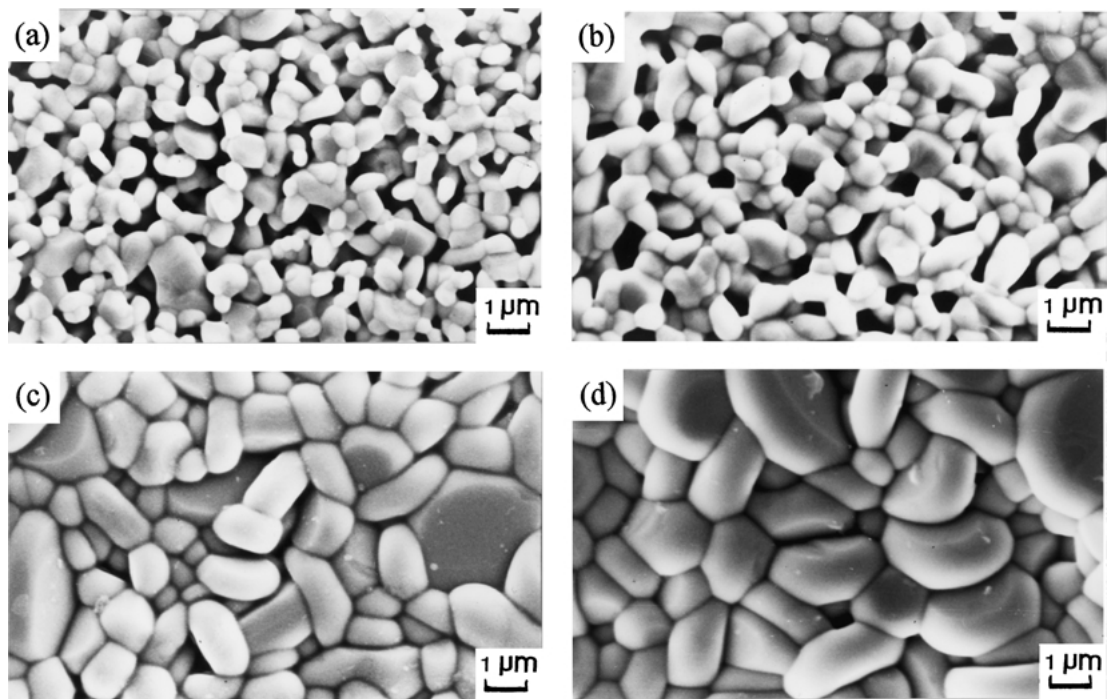


Figure 3 Microstructures of the ceramics with $x = 0$ sintered at (a) 1000°C, (b) 1100°C, (c) 1200°C, and (d) 1300°C.

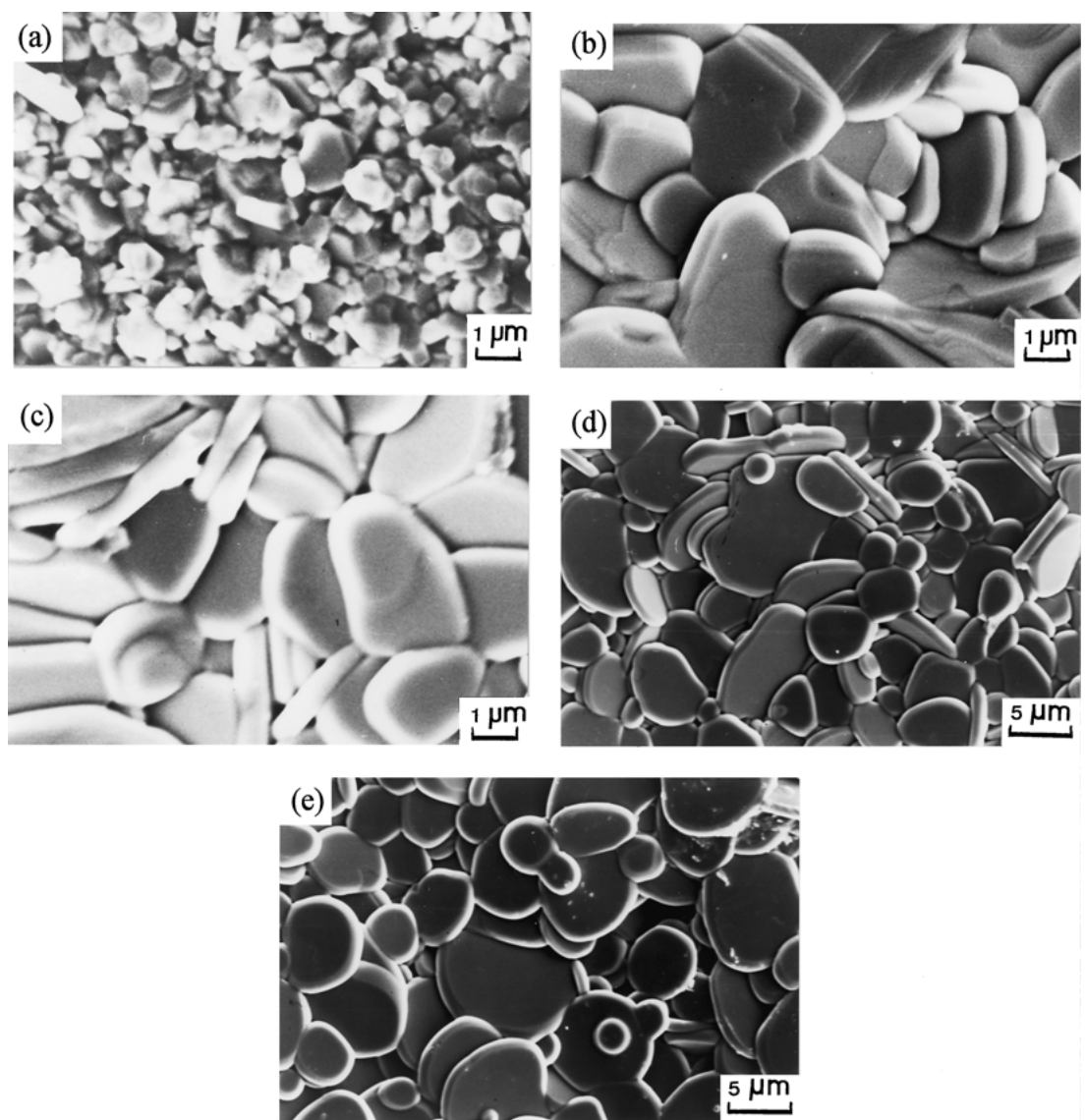


Figure 4 Typical microstructures of the doped ceramics. (a)–(d): $x = 0.05$ sintered at (a) 1000°C, (b) 1100°C, (c) 1200°C, (d) 1300°C, and (e): $x = 0.2$ sintered at 1300°C.

low (900°–1000°C), and increased smoothly when the sintering temperature is high (1100°–1300°C) (compare Fig. 4e for $x = 0.2$ with Fig. 4d for $x = 0.05$).

The above described microstructure development might explain the density result shown in Fig. 2. The density reduction at $\geq 1100^\circ\text{C}$ for each doped composition should be caused by the abrupt increase in grain-size and the fully developed plate-like-grained microstructure. The densification process is usually inhibited by rapid grain growth. Moreover, the plate-like grains with a high aspect ratio, when impinge each other, might also suppress the densification process due to the large growth-rate anisotropy. Evidence supporting this hypothesis is that the undoped composition does not show density reduction because no abrupt increase in grain size occurs and the plate-like-grained microstructure is not fully developed.

3.2. Dielectric properties and ferroelectric properties

The dielectric constant (κ') at 1 kHz as a function of sintering temperature is shown in Fig. 5a. All compositions showed a maximum κ' when the ceramics were sintered at 1200°C (undoped) or 1000°C (doped). The κ' -value of the undoped composition first increased from 90 to

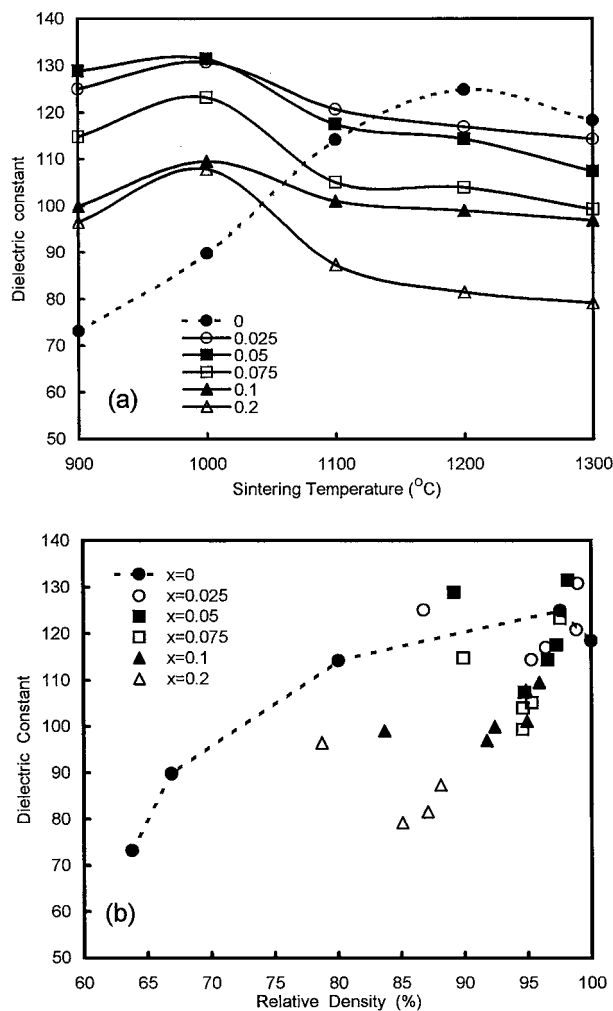


Figure 5 Dielectric constant at 1 kHz as a function of (a) sintering temperature and (b) relative density.

125 in the temperature range 1000°–1200°C, mainly due to the increase in relative density from 67% to 97%, followed by a slight decrease in κ' to 120 at 1300°C. In comparison with the undoped composition, the κ' reduction for the doped compositions is more significant and shifts to a lower sintering temperature ($\geq 1100^\circ\text{C}$). As a result, as compared with the undoped composition, the κ' -value increased when the sintering temperature was $\leq 1000^\circ\text{C}$, while the κ' -value decreased when the sintering temperature was $\geq 1000^\circ\text{C}$. Moreover, for the doped compositions, the κ' -value generally decreased with the increase in the vanadium content.

The above trend of κ' is quite similar with that of densification (Fig. 2), indicating that κ' should be at least influenced by densification. Fig. 5b shows the variation of κ' with relative density. Consider the ceramics with relative density $\geq 90\%$, it was found that the data points located above the curve for $x = 0$ are associated with the ceramics with $x = 0.025$ – 0.05 sintered at 900°–1000°C. However, the data points located below the curve for $x = 0$ are associated with the ceramics with $x = 0.025$ – 0.05 sintered at $\geq 1100^\circ\text{C}$ and the ceramics with $x \geq 0.075$. It is suggested that the increased κ' for the lower sintering temperature (900°–1000°C) and lower vanadium content might be caused by the “intrinsic” effect of vanadium doping. Namely, doping of vanadium will increase κ' if the effects of microstructure (porosity, grain size, second phase, etc.) can be eliminated. On the other hand, the reduced κ' for the higher sintering temperature ($\geq 1100^\circ\text{C}$) and higher vanadium content is possibly caused by the density reduction (Fig. 2), the slight increase in the content of second phase (Fig. 1), the increase in the preferred orientation (Fig. 1), and/or the increased grain-size (Fig. 4). It is also noted from Fig. 5b that for the doped ceramics with relative density $\geq 90\%$, the κ' -value is in the range of 100–130. The dielectric loss tangent ($\tan \delta$) for the ceramics with relative density $\geq 90\%$ is below 1%.

Fig. 6a shows the typical P - E hysteresis loops for the undoped ceramics. The loop is slim and non-saturated, until the sintering temperature is $\geq 1200^\circ\text{C}$, mainly due to poor densification. The P_r - and E_C -values decreased from 16 $\mu\text{C}/\text{cm}^2$ and 72 kV/cm for 1200°C to 8.9 $\mu\text{C}/\text{cm}^2$ and 60 kV/cm for 1300°C. However, saturated loops can be observed for the doped ceramics sintered at much lower temperatures, as shown typically in Fig. 6b and c for $x = 0.025$. The variations of P_r and E_C with the sintering temperature are shown in Fig. 7a and b, respectively. It can be seen from Fig. 7a that the undoped composition showed an optimum sintering temperature (1200°C) for maximum P_r . For the compositions with $x = 0.025$ – 0.075 , the optimum sintering temperature was lowered to 1000°C and the maximum P_r value was remarkably increased. When the vanadium content (x) was further increased to 0.1–0.2, the maximum disappeared. As compared with the undoped composition, the P_r -value was improved when the sintering temperature was $\leq 1100^\circ\text{C}$, while the P_r -value was reduced when the sintering temperature was $\geq 1200^\circ\text{C}$. According to Fig. 7b, the undoped composition revealed a maximum E_C at 1000°C while the doped compositions revealed a minimum E_C at 1000°C. Moreover,

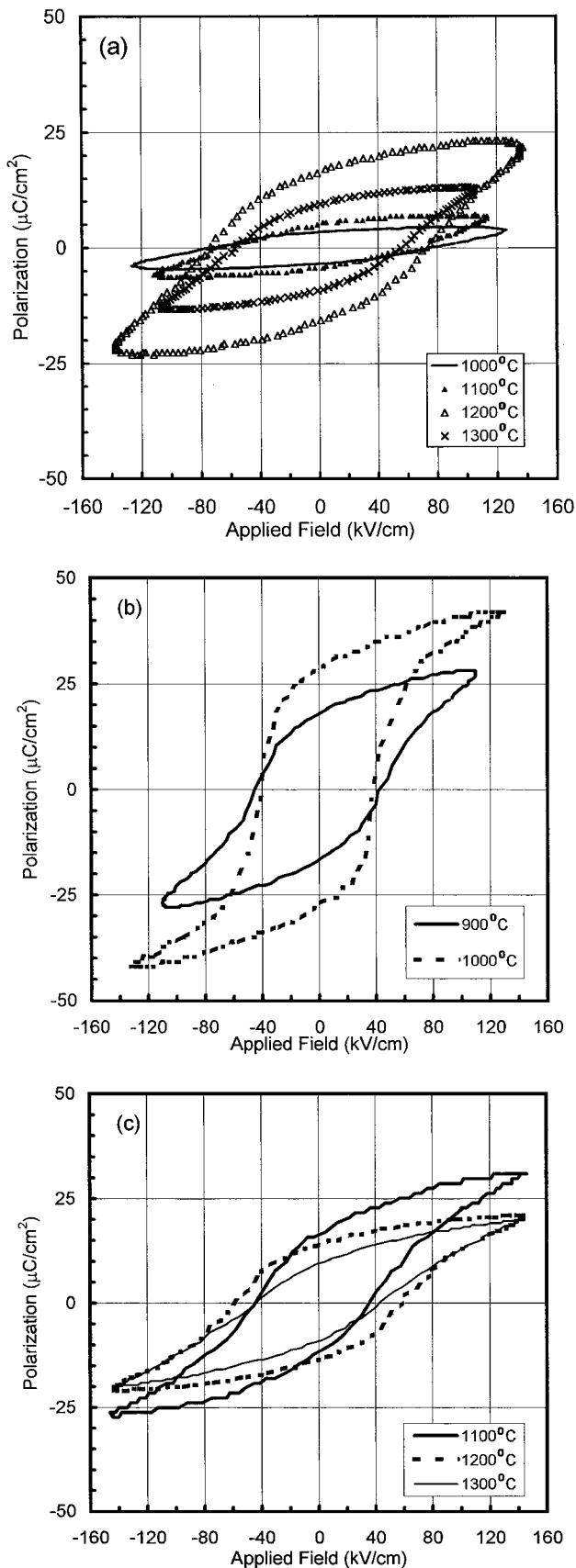


Figure 6 P-E hysteresis loops of the ceramics with $x =$ (a) 0, (b) and (c) 0.025.

the P_r - and E_C -value for the doped compositions generally decreased and increased, respectively, with the increase in the vanadium content. As a result, there are an optimum sintering temperature of 1000°C and an optimum vanadium content of $x = 0.025$ for maximum P_r and minimum E_C . As compared with the

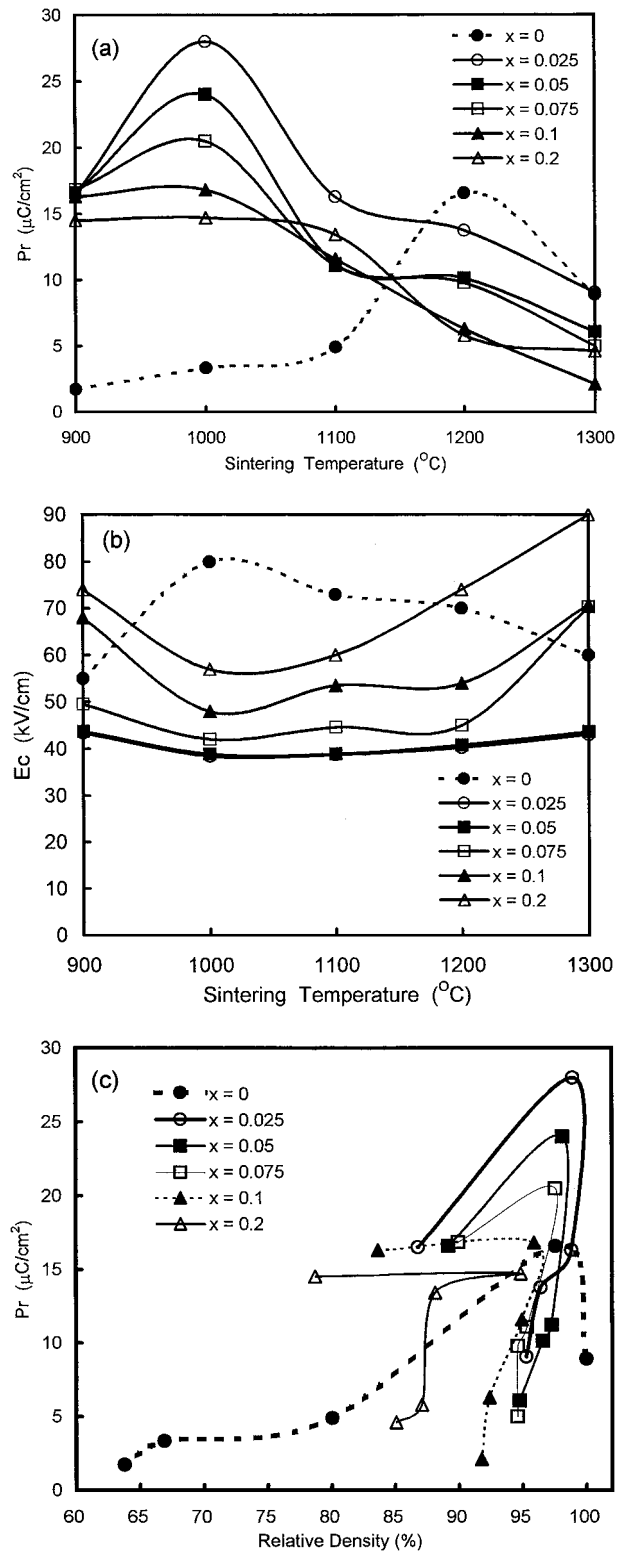


Figure 7 Variations of (a) P_r and (b) E_C as a function of sintering temperature. (c) Variation of P_r as a function of relative density.

undoped ceramics, the ferroelectric properties can be significantly improved by doping with an appropriate amount of vanadium and sintering at 1000°C.

It is noted that the trend of P_r is similar to that of dielectric constant (Fig. 5a) and densification (Fig. 2), indicating that P_r should at least be influenced by densification. Watanabe *et al.* [17] has shown that the dependence of P upon Sr content in isomorphous strontium bismuth niobate (SBN) and SBT can be explained by the dependence of grain orientation to Sr content. In

the present study, the *c*-axis orientation of the undoped and doped samples were vanished when the samples surface were polished (Section 3.1), and the polished samples were used for dielectric and ferroelectric measurements. Therefore, the effect of sample orientation is excluded. Fig. 7c shows the variation of P_r with relative density. Consider the ceramics with nearly the same density (e.g., around 95–100%), it was found that the data points located above and below the curve for $x = 0$ are associated with the ceramics sintered at 1000°C and 1100–1300°C, respectively. Similar to that discussed for the k' data (Fig. 5b), it is suggested that the increased P_r for the lower sintering temperature might be caused by the “intrinsic” effect of vanadium doping. It has been reported that partial substitution of Nb^{5+} in $SrBi_2Nb_2O_9$ ceramic by a smaller cation V^{5+} can improve the ferroelectric properties [18], due to the enlarged rattling space. This factor might explain the improved P_r value of the present $SrBi_2Ta_2O_9$ materials sintered at lower temperatures. On the other hand, the decrease in P_r for higher vanadium content and higher sintering temperatures (Fig. 7a and c) might be caused by the density reduction (Fig. 2), the slight increase in the amount of second phase (Fig. 1), and/or the rapid coarsening in microstructure (Fig. 4).

4. Conclusions

The effects of vanadium doping on the densification, microstructure, and properties of $SrBi_2(Ta_{1-x}V_x)_2O_9$ ceramics were investigated, with the following results:

1. Single layered perovskite was formed in the undoped ceramics. For the doped ceramics, a trace amount of second phase formed when the vanadium content and the sintering temperature were increased.

2. For the doped ceramics, the densification and grain-growth processes were shifted to a lower temperature range. The densification was reduced when the sintering temperature is higher or when the vanadium content is increased, possibly caused by the abrupt increase in grain size and the fully developed plate-like-grained microstructure.

3. For the ceramics with relative density $\geq 90\%$, the dielectric constant is 120–125 and 100–130 for the un-

doped and doped ceramics, respectively, and the dielectric loss tangent is below 1%.

4. As compared with the undoped ceramics, the ferroelectric properties can be significantly improved by doping with an appropriate amount of vanadium and sintering at 1000°C.

5. The variations of dielectric and ferroelectric properties are influenced by the incorporation of vanadium into crystal lattice and several microstructural factors (such as densification, content of second phase, preferred orientation, and the size and shape of grains).

References

1. C. A. PAZ de ARAUJO, J. D. CUCHIARO, L. D. McMILLAN, M. C. SCOTT and J. F. SCOTT, *Nature* (London) **374** (1995) 27.
2. S. B. DESU and T. LI, *Mater. Sci. Eng. B* **34** (1995) 4.
3. S. B. DESU and D. P. VIJAY, *ibid.* **32** (1995) 83.
4. J. F. SCOTT, in “Thin Film Ferroelectric Materials and Devices,” edited by R. Ramech (Kluwer, Norwell, MA, 1997) p. 115.
5. *Idem.*, *Ann. Rev. Mater. Sci.* **28** (1998) 79.
6. S. BHATTACHARYYA, A. R. JAMES and S. B. KRUPANIDHI, *Solid State Comm.* **108** (1998) 759.
7. T. NOGUCHI, T. HASE and Y. MIYASAKI, *Jpn. J. Appl. Phys.* **35** (1996) 4900.
8. S. KOJIMA and I. SAITOH, *Physic B* **263–264** (1999) 653.
9. Y. TORII, K. TATO, A. TSUZUKI, H. J. HWANG and S. K. DEY, *J. Mater. Sci. Lett.* **17** (1998) 827.
10. M. MIURA and M. TANAKA, *Jpn. J. Appl. Phys.* **37** (1998) 2554.
11. H. WATANABE, T. MIHARA, H. YOSHIMORI and C. A. P. ARAUJO, *ibid.* **34** (1995) 5240.
12. M. A. RODRIGUEZ, T. J. BOYLE, B. A. HERNANDEZ, C. D. BUCHHEIT and M. O. EATOUGH, *J. Mater. Res.* **11** (1996) 2282.
13. C. LU and C. WEN, *Mater. Res. Soc. Symp. Proc.* **541** (1999) 229.
14. B. AURIVILLIUS, *Ark. Kemi.* **1** (1949) 463.
15. R. D. SHANNON and C. T. PREWITT, *Acta. Cryst. B* **25** (1969) 925.
16. J. J. BROWN, in “Phase Diagrams for Ceramists,” vol. IV, edited by G. Smith (The American Ceramic Society, Columbus, Ohio, USA, 1981) Fig. 5182.
17. K. WATANABE, M. TANAKA, E. SUMITOMO, K. KATORI, H. YAGI and J. F. SCOTT, *Appl. Phys. Lett.* **73** (1998) 126.
18. Y. WU and G. CAO, *J. Mater. Sci. Lett.* **19** (2000) 267.

Received 12 March

and accepted 10 October 2002